Author Manuscript

Author Manuscript

Author Manuscript

Author Manuscript

HHS Public Access

Author manuscript

Hepatology. Author manuscript; available in PMC 2016 November 01.

Published in final edited form as:

Hepatology. 2015 November ; 62(5): 1536–1550. doi:10.1002/hep.27998.

A novel "humanized mouse" model for autoimmune hepatitis and the association of gut microbiota with liver inflammation

Muhammed Yuksel[1,2,8,*], **Yipeng Wang**[1,3,*], **Ningwen Tai**[1], **Jian Peng**[1], **Junhua Guo**[1,4], **Kathie Beland**[5], **Pascal Lapierre**[6], **Chella David**[7], **Fernando Alvarez**[5], **Isabelle Colle**[2], **Huiping Yan**[3], **Giorgina Mieli-Vergani**[8], **Diego Vergani**[8], **Yun Ma**[8], and **Li Wen**[1,9]

[1]Section of Endocrinology, Yale University School of Medicine, New Haven, USA

[2]Laboratory of Hepatology and Gastroenterology, Ghent University, Belgium

[3]Clinical Research Centre for Autoimmune Liver Disease, Beijing You-an Hospital, Capital Medical University, Beijing, China

[4]Department of Rheumatology, PLA General Hospital, Beijing, China

[5]Division of Gastroenterology, Hepatology and Nutrition, Sainte-Justine University Hospital, Montreal, Canada

[6]Immunovirology Laboratory, Institut national de la recherche scientifique, INRS-Institut Armand-Frappier, Laval, Québec, Canada

[7]Department of Immunology, Mayo Clinic, Minnesota, USA

[8]Institute of Liver Studies, King's College London Faculty of Life Sciences and Medicine at King's College Hospital, London, UK

Abstract

Background—Autoimmune hepatitis (AIH) in humans is a severe inflammatory liver disease, characterized by interface hepatitis, the presence of circulating autoantibodies and hyper-gammaglobulinemia. There are two types of AIH, type-1 (AIH-1) and type-2 (AIH-2) characterized by distinct autoimmune serology. Patients with AIH-1 are positive for anti-smooth muscle and/or anti-nuclear (SMA/ANA) autoantibodies whereas patients with AIH-2 have anti-liver kidney microsomal type 1 (anti-LKM1) and/or anti-liver cytosol type 1 (anti-LC1) autoantibodies. Cytochrome P4502D6 (CYP2D6) is the antigenic target of anti-LKM1 and formiminotransferase cyclodeaminase (FTCD) is the antigenic target of anti-LC1. It is known that AIH, both type-1 and type-2, is strongly linked to the Human Leukocyte Antigen (HLA) alleles -DR3, -DR4 and -DR7. However, the direct evidence of the association of HLA with AIH is lacking.

Methods—We developed a novel mouse model of AIH using the HLA-DR3 transgenic mouse on the non-obese diabetic (NOD) background (HLA-DR3 NOD) by immunization of HLA-DR3^{-}

[9]Corresponding author: Li Wen, Section of Endocrinology, Yale University School of Medicine, Mail Box-208020, New Haven, CT-06520, USA, Tel: 203-785-7186, Fax: 203-737-5558, li.wen@yale.edu.

*These authors contributed equally to the study

Author Manuscript Author Manuscript Author Manuscript Author Manuscript

and HLA-DR3$^+$ NOD mice with a DNA plasmid, coding for human CYP2D6/FTCD fusion protein.

Results—Immunization with CYP2D6/FTCD leads to a sustained elevation of alanine aminotransferase (ALT), development of ANA and anti-LKM1/anti-LC1 autoantibodies, chronic immune cell infiltration and parenchymal fibrosis on liver histology in HLA-DR3$^+$ mice. Immunized mice also showed an enhanced Th1 immune response and paucity of the frequency of regulatory T-cell (Treg) in the liver. Moreover, HLA-DR3$^+$ mice with exacerbated AIH showed reduced diversity and total load of gut bacteria.

Conclusion—Our humanized animal model has provided a novel experimental tool to further elucidate the pathogenesis of AIH and to evaluate the efficacy and safety of immunoregulatory therapeutic interventions *in vivo*.

Keywords

autoimmunity; mouse model; regulatory T-cells; gut bacteria

Introduction

Autoimmune hepatitis (AIH) is a severe form of liver disorder. Similar to many types of autoimmune diseases, it affects more females than males and is characterized by increased aspartate aminotransferase (AST) and alanine aminotransferase (ALT), serologically by the presence of autoantibodies and increased levels of immunoglobulin-G (IgG) and histologically by interface hepatitis (1–3). There are two types of AIH, type-1 (AIH-1), positive for anti-smooth muscle (SMA) and/or anti-nuclear antibodies (ANA), and type-2 (AIH-2), positive for anti-liver-kidney microsomal type-1 (anti-LKM1) and/or anti-liver cytosol type-1 (anti-LC1) antibodies (4), though some AIH-2 patients are also positive for ANA (5). The autoantigen of anti-LKM1 has been identified as cytochrome P4502D6 (CYP2D6) (6), whereas anti-LC1 recognizes formiminotransferase cyclodeaminase (FTCD) (7), both autoantigens are expressed in hepatocytes. Previous studies suggested that anti-LKM1 and anti-LC1 may contribute to the autoimmune destruction of the liver (6, 7). Genetically, AIH-1 is strongly associated with genes encoding for human leukocyte antigen (HLA) class II DR3 (8, 9) and DR4 (10, 11), while AIH-2 is associated with the possession of DR3 and DR7 (12). HLA-DR3, therefore, is a genetic determinant of both types of AIH. Moreover, HLA-DR3 is also associated with other autoimmune disorders including systemic lupus erythematosus (13, 14) and type-1-diabetes (15, 16).

Though AIH was described over 70 years ago (17), the immunopathogenesis of the disease still remains unclear. We and others have shown that hepatocyte destruction in AIH is mediated by a Th1 immune response, but how the hepatic immune tolerance breakdown and what the role of genetic suceptiblity genes in tolerance breakdown are not fully understood. Lack of an appropriate animal model of human AIH has hindered our understanding of the immunopathogenesis of the disease. This has resulted in a delay in the discovery of more specific modes of treatment to replace the currently used immunosuppressive therapy, which is usually for life and can cause severe side effects. The stimuli used in some early animal models of AIH were non-liver specific, which might explain the development of only mild

Author Manuscript Author Manuscript Author Manuscript Author Manuscript

and/or transient biochemical and histological changes (18, 19). More recent studies have shown that immunization with liver autoantigens can induce liver damage similar to human AIH, though the disease course and the biochemical and/or histological features fall short of mirroring it faithfully (20–23). To study the role of autoimmune suceptibility genes, in particular HLA-DR3, we generated human HLA-DR3 transgenic mouse on the non-obese diabetic (NOD) genetic background, which harbors numerous autoimmune susceptibility genes, such as IL-2 receptor, PTPN22 and CTLA-4 (24–26). Immunization of HLA-DR3 NOD mice with liver autoantigen CYP2D6/FTCD encoding plasmid DNA leads to autoimmune liver damage with i) elevated ALT; ii) interface hepatitis and fibrosis; iii) enhanced Th1 and Th17 T-cell responses and iv) the production of ANA and anti-LKM1/anti-LC1 autoantibodies. Moreover, these mice have reduced frequency of liver $CD4^+CD25^+Foxp3^+$ T regulatory cells (Treg). Our results show that HLA-DR3 NOD mice do faithfully mirror human AIH. This novel mouse model of human AIH can be used for elucidating the pathogenesis of the disaese and for pre-clinical testing of immunotherapies *in vivo*.

Materials and Methods

Animals

Wild type (WT) NOD mice were obtained originally from the Jackson Laboratories (Bar Harbor, ME, USA) and maintained at Yale animal facility for nearly 30 years. HLA-DR3 transgenic NOD mice were generated by back-crossing HLA-DR3 C57BL/10 mice (27) to the NOD background for >10 generations. All the mice used in this study were 6–10 weeks old and housed in specific-pathogen–free (SPF) conditions with autoclaved food and bedding in individually-ventilated filter cages. All the studies were approved by the Institutional Animal Care and Use Committee of Yale University.

Reagents

Generation of CYP2D6/FTCD DNA construct has been reported previously (20). The plasmid DNA was transferred to *E coli* competent cells and purified with endotoxin-free plasmid purification kit (Qiagen, Valencia, CA, USA) after overnight culture. CpG-ODN (2395, type C) was synthesized by Keck Facility at Yale University. All the monoclonal antibodies (mAbs) used in this study were purchased from BioLegend or eBioscience (San Diego, CA, USA).

Immunization and liver histology

CYP2D6/FTCD plasmid DNA (100 μg/mouse) together with CpG-ODN 2395 as an adjuvant (75μg/mouse) in PBS were emulsified with an equal volume of Incomplete Freund's Adjuvant (IFA, Sigma, USA). HLA-DR3 NOD mice were immunized with 100μl of the above antigen mix by intraperitoneal injection. A separate group of HLA-DR3 NOD mice were injected with CpG-ODN and IFA as control. We also immunized two groups of HLA-DR3 transgene negative NOD mice with antigen mixture or adjuvant control. All the mice were boosted twice with a 2-week interval. The experiment was terminated 6 month after primary immunization. Liver tissue was fixed in 4% phosphate buffered formaldehyde and embedded in paraffin and assessed blindly, using the METAVIR score (28) and the

Author Manuscript Author Manuscript Author Manuscript Author Manuscript

Ishak modified (mISHAK) histological activity scoring system (29). Tissue sections were stained with haematoxylin-eosin, Sirius-Red or Methyl-green-pyronin to investigate liver inflammation, fibrosis or plasma cell infiltration respectively. None of the mice used in the study developed diabetes.

Measurement of serum alanine aminotransferase (ALT)

The level of serum ALT was measured using an ALT kit (Cayman Chemical, Ann Arbor, MI, USA) according to the manufacturer's instructions.

Liver autoantibody specific Enzyme-Linked Immunosorbent Assay (ELISA)

ANA was tested by indirect immunofluorescence assay on tissue mosaic slides (Euroimmun, Lübeck, Germany) using fluorescence microscopy. Anti-LKM1/anti-LC1 autoantibodies were measured by ELISA as described by Lapierre (30). Briefly, the fusion protein produced by the pMAL-cR1-CYP2D6-FTCD plasmid (human CYP2D6/FTCD) was purified and used as antigen in the ELISA (0.2μg/well). An antiserum was considered positive if the optical density (OD) reading was over 2 times higher than the mean OD of the pre-immune mice serum sample, which was then converted to the serum dilution at the positive OD readings. Serum samples were diluted from 1:50 to 1:400.

Isolation of mononuclear cells and flow cytometry

Prior to tissue harvesting, mouse liver was first perfused with sterile PBS via the portal vein and weighed. After homogenizing the liver tissue, liver mononuclear cells (LMNCs) were harvested at the interface of a 40% and 80% Percoll (GE Healthcare, Piscataway, NJ, USA) by discontinuous gradient centrifugation. Residual red blood cells (RBC) were lysed with RBC lysis buffer (eBioscience). The LMNCs were then washed with PBS before staining with mAbs. The splenocytes (SMNCs) were obtained after homogenization and lysis of RBCs with lysing buffer and stained with mAbs. The expression of different surface markers and intracellular cytokines (ICC) in LMNCs or SMNCs was analyzed by flow cytometry as described previously (31). Bone marrow dendritic cells (BMDC) were generated as described previously (32).

T-cell purification and proliferation assay

Splenic $CD4^+$ T-cells were purified using negative selection by magnetic beads. Briefly, total splenocytes were incubated on ice for 30 min with anti-CD8 T-cell (TIB-105, to remove $CD8^+$ T-cells), and anti-IA^{g7} (10.2.16) to remove MHC-class-II^+ macrophages and DCs. After washing, the cells were incubated with magnetic beads conjugated with anti-rat IgG (all the above mAbs are of rat origin) and anti-mouse IgM and IgG (to remove B-cells) for 45 min on ice. Non $CD4^+$ T-cells were removed by a magnetic separation. The purity of $CD4^+$ T-cells was routinely over 90% as examined by flow cytometry.

Antigen specific $CD4^+$ T-cell responses were tested by culturing purified splenic $CD4^+$ T-cells (10^5/well) with irradiated BMDC (10^4/well) in the presence or absence of CYP2D6/FTCD plasmid DNA or a mix (1:1) of two peptides, $CYP2D6_{313-332}$ and $CYP2D6_{393-412}$ (3μg/ml), which are known to be HLA-DR3 restricted (33, 34) for 4-days. ^{3}H-thymidine was added during the last 16 hours of the 4-day culture. T-cell proliferation was evaluated by ^{3}H-

Author Manuscript Author Manuscript Author Manuscript Author Manuscript

thymidine incorporation in a beta plate counter (Perkin Elmer Wallace, Ohio, USA). We also performed antigen-nonspecific T-cell proliferation assays, in which T-cells were stimulated with anti-CD3 with or without anti-CD28 antibody. All the proliferation assays were performed in triplicates.

Treg suppression assay

To test the function of Treg cells, we evaluated the suppression of mixed lymphocyte reaction (MLR). NOD splenocytes (1×10^5/well) were stimulated with irradiated C57BL/6 splenocytes (5×10^4/well) in the absence or presence of Treg cells ($CD4^+CD25^+$, 1.25×10^4/well) purified using a Treg purification kit (StemCell Technology), from WT or HLA-DR3 spleens. MLR was measured by ^{3}H-thymidine incorporation at the end of a 4-day culture. The suppression of MLR by Treg cells was calculated as the percentage of inhibition of MLR.

Serum immunoglobulin assay

Serum immunoglobulin (Ig) levels of different isotypes were determined by ELISA. All the reagents for Ig detection were purchased from Southern Biotechnology (Birmingham, AL, USA). The samples were diluted at 1:1,000 and assayed in triplicates. ELISA plates were read on a 1420 Multilabel Counter (Perkin Elmer, Ohio, USA).

Real-time PCR

RNA from 10 mg liver tissue was isolated with E.Z.N.A.® total RNA kit (Omega Biotek), according to the manufacturer's instructions. Two μg of RNA were reversely transcribed to cDNA with oligo(dT) primer together with dNTP and the SuperScript®III reverse transcriptase (Invitrogen, Carlsbad, CA). The cDNA was used for real time PCR in the presence of SYBR green. All the samples were run in duplicate and mean values were used for analysis. The primer sequences are; α-sma-: forward (f)-ccagcaccatgaagatcaag-, reverse (r)-tggaaggtagacagcgaagc-, lox: f-tcactgcgctcgttctgat-, r-cgatcgaaagtatgagggatg-, loxl2: f-cctacaaccccaaagcctataa-, r-cgtgcagttcatagaaaacttcc-, tgf-β: f-agcccgaagcggactactat, r-ttcccgaatgtctgacgtatt, gapdh: f-tgtagaccatgtagttgaggtca, r-aggtcggtgtgaacggatttg. The relative mRNA levels of the α-SMA, LOX, LOXL2 and TGF-β were determined using the $2^{-\Delta\Delta Ct}$ method by normalization with the house-keeping gene GAPDH.

Gut bacterial DNA isolation and 16S rRNA gene sequencing

Gut bacterial DNA isolation and 16S rRNA sequencing was performed as previously described (35). Briefly, total bacterial DNA was extracted from 0.25g fecal sample using the bead beating method described by Favier (36) with modifications. After purification, the V2 region of the 16S rRNA gene was used to amplify each DNA sample using a composite broadly conserved bacterial forward primer (5′-CATGCTGCCTCCCGTAGGAGT-3′) and bar-coded broad-range bacterial reverse primer (5′-TCAGAGTTTGATCCTGGCTCAG-3′) (35). The PCR products were purified with a Qiagen (Valencia, CA, USA) gel extraction kit and quantified by NanoDrop. Each sample was then diluted to a concentration of 1×10^9 molecules/μl in TE buffer and pooled. The pooled sample was pyrosequenced with the GS-Titanium-454 sequencing system according to the manufacturer's instructions (Roche 454,

Author Manuscript Author Manuscript Author Manuscript Author Manuscript

Life Sciences Corp, Branford, CT, USA). The sequencing data were analyzed with QIIME software package (version 1.6) (37) to assign operational taxonomic units (OTUs). Taxonomy assignment was performed at various levels using representative sequences of each OTU.

Statistical Analysis

Statistical analysis was performed using GraphPad Prism 5 software. Non-parametric two-way ANOVA or Student's t-test was used in most experiments and P values <0.05 were considered significant.

Results

HLA-DR3 NOD mice were susceptible to CYP2D6/FTCD induced liver injury

To test whether HLA-DR3 NOD mouse could be used as an AIH model, we immunized the mice with CYP2D6/FTCD plasmid DNA in adjuvant (CpG+IFA, n=9). We also injected HLA-DR3 NOD mice with adjuvant only as controls (n=7). To investigate if HLA-DR3 contributes to AIH induction, we immunized two groups of WT NOD mice with CYP2D6/FTCD in adjuvant or adjuvant alone (n=8/group). Serum ALT was monitored monthly. ALT was significantly elevated in HLA-DR3 NOD mice 3 months after immunization with autoantigen (Fig. 1A), whereas ALT levels remained normal in all the control groups. HLA-DR3 mice immunized with autoantigen showed the highest level of ALT compared to all controls at 6 months after immunization (Fig. 1A). Though WT NOD mice immunized with CYP2D6/FTCD also showed a mild elevation of ALT four months after immunization with a further elevation at six months, remaining significantly lower than those in the HLA-DR3 counterparts (Fig. 1A).

HLA-DR3 NOD mice developed anti-nuclear and anti-LKM1/anti-LC1 autoantibody after immunization

To investigate whether CYP2D6/FTCD induced liver injury in HLA-DR3 NOD mice was accompanied by autoantibody production; we tested ANA, anti-LKM1 and anti-LC1 autoantibodies. We found that HLA-DR3 mice developed higher ANA autoantibodies after CYP2D6/FTCD immunization compared to WT NOD and HLA-DR3 NOD control mice (Fig. 1B). Interestingly, both antigen immunized WT and HLA-DR3 NOD mice developed anti-LKM1/anti-LC1 autoantibodies, although the anti-LKM1/anti-LC1 titer was significantly higher in the antigen immunized HLA-DR3 mice than control HLA-DR3 NOD mice, while the difference was not significant in the WT NOD mice (Fig. 1C).

HLA-DR3 NOD mice had increased mononuclear cell infiltration in the liver after immunization

To examine whether liver injury induced by CYP2D6/FTCD immunization resulted in liver enlargement, we weighed the liver when the mice were terminated. The liver weight was slightly higher in HLA-DR3 NOD mice immunized with autoantigen, although this was not significant (Fig. 1D). We next investigated liver immune cells in all 4 groups of mice. As shown in Fig. 1E, the absolute number of LMNC per gram liver weight was significantly higher in HLA-DR3 NOD mice immunized with autoantigen compared to control mice

Author Manuscript Author Manuscript Author Manuscript Author Manuscript

immunized with adjuvant only. WT NOD mice immunized with autoantigen also showed an increased number of LMNCs compared to the WT NOD mice injected with adjuvant only (Fig. 1E). However, HLA-DR3 NOD mice had the highest number of LMNC after CYP2D6/FTCD immunization (Fig. 1E).

HLA-DR3 NOD mice experienced more severe liver damage after immunization

To investigate whether HLA-DR3 NOD mice develop liver damage histologically similar to patients with AIH, we analyzed their liver pathology. We found mild immune cell infiltration in both WT and HLA-DR3 NOD mice immunized with adjuvant (Fig. 2A, control). However, CYP2D6/FTCD immunization led to more severe immune cell infiltration (Fig. 2A, CYP2D6/FTCD), especially in DR3 positive mice. Importantly, we found patches of necrotic liver tissue in HLA-DR3 NOD mice immunized with CYP2D6/FTCD (supplementary Fig. 1A), while this was not seen in WT NOD mice after immunization with the same antigen (Fig. 2A). The mice in the control immunized groups showed some mild inflammation (Fig. 2A). Furthermore, we found stage F1/F2 mild liver fibrosis based on the METAVIR score, in 50% of HLA-DR3 and ~25% WT NOD mice immunized with CYP2D6/FTCD (Fig. 2B), albeit this difference did not reach a statistical significance. In addition, there was no fibrosis found in control immunized mice (data not shown). Next, we analyzed fibrosis related genes including α-SMA, Lox, LoxL2 and TGF-β (38) in liver tissues by qPCR. Consistent with the histopathology, we did not find statistical significance between immunized HLA-DR3 mice and the controls, although there was a clear trend of increased expression of LoxL2 and TGF-β in the immunized HLA-DR3 mice (supplementary Fig. 1B). Furthermore, the necrosis-inflammation score of the liver mISHAK showed that HLA-DR3 NOD mice immunized with antigen had more severe liver damage compared to the antigen immunized WT NOD group (Fig. 2C). In addition, we found that significantly more plasma cells, a hallmark of AIH, were present in portal fields of antigen immunized HLA-DR3. Interestingly, antigen immunized WT NOD mice also showed plasma cell infiltration compared to their control immunized counterparts (Fig. 2D +E).

HLA-DR3 NOD mice had increased hepatic T-cells but decreased Foxp3$^+$ Tregs after immunization

Next, we examined the composition of liver infiltrated immune cells by flow cytometry. There was a significant increase of CD4$^+$ and CD8$^+$ T-cells, both in frequency and absolute numbers, within the infiltrated hepatic inflammatory cells in HLA-DR3 NOD mice immunized with autoantigen whereas the numbers of B-cells, macrophages and dendritic cell were similar to control immunized mice (Fig. 3A). We also analyzed the effect of CYP2D6/FTCD immunization and liver injury on regulatory T-cells and found a significant decrease of Foxp3$^+$ Tregs frequency in LMNC from the HLA-DR3 NOD mice immunized with CYP2D6/FTCD compared to the control (adjuvant only) (Fig. 3B). This reduction appeared only in the liver, as the frequency of Tregs in spleen remained unchanged (data not shown). However, when we analyzed absolute Treg cell number/gram liver tissue, we found that in the CYP2D6/FTCD immunized mice, whether WT or HLA-DR3, more Tregs were present than in immunized mice (Fig. 3C). This was also restricted to the liver (data not shown). We then investigated the suppressive function of Treg cells in a mixed lymphocyte

Author Manuscript Author Manuscript Author Manuscript Author Manuscript

reaction (MLR). Total splenocytes from naïve WT NOD mice were co-cultured with irradiated splenocytes from C57BL/6 mice in presence or absence of purified splenic Treg cells from naïve WT or HLA-DR3 NOD mice. The suppressive function of Treg cells from HLA-DR3 NOD mice was impaired compared to their counterparts from WT NOD mice; adding Treg cells from HLA-DR3 NOD mice in the MLR did not significantly suppress the allo-reaction (Fig. 3D+E).

HLA-DR3 NOD mice increased numbers of inflammatory cytokine-producing T-cells in the liver after immunization

To determine if there were any functional changes within LMNCs in response to autoantigen immunization, we examined their post-immunization cytokine profile. We found that there was a significant decrease in IL-4 producing $CD4^+$ T-cell number in LMNCs from HLA-DR3 mice after antigen immunization compared to the control HLA-DR3 mice (Fig. 4 A +B). In contrast, IL-17 producing $CD4^+$ T-cells were significantly increased in the autoantigen-immunized mice compared with the control group (Fig. 4 C+D). Inflammatory cytokine-producing $CD8^+$ T-cells were also significantly increased (Fig. 4 E+F and G+H, for IFN-γ and TNF-α producing $CD8^+$ T-cells, respectively). There was a trend towards an increase for another inflammatory cytokine, IL-6, by T-cells, macrophages and DCs but this did not reach statistical significance (data not shown). We did not find any difference in the immunoregulatory cytokine IL-10-producing immune cells among all the groups analyzed (data not shown).

T-cells from HLA-DR3 NOD mice responded to CYP2D6/FTCD *in vitro* after immunization

To investigate the CYP2D6/FTCD autoantigen specific T-cell response, we performed proliferation assays following CYP2D6/FTCD plasmid stimulation using purified splenic or hepatic $CD4^+$ T-cells from HLA-DR3 positive and negative mice immunized with the autoantigen. Splenic T-cells showed significant response to the antigen in immunized HLA-DR3 positive, but not negative mice (Fig. 5A), however, most of the hepatic $CD4^+$ T-cells, regardless the origin, underwent activation induced cell death (data not shown). We further tested the $CD4^+$ T-cell response to two HLA-DR3 restricted CYP2D6 peptides (33) and found that both hepatic (Fig. 5B) and splenic (Fig. 5C) $CD4^+$ T-cells from HLA-DR3 mice responded to the peptide. To test if there was an intrinsic functional difference in T-cells between the two types of mice, we stimulated total splenic T-cells with anti-CD3 with or without anti-CD28. As shown in (Fig. 5D+E), there was no difference in T-cell response to anti-CD3, indicating that the introduction of HLA-DR3 transgene does not alter T-cell function and indirectly supporting the antigen specificity of the T-cell response to CYP2D6.

B-cells from HLA-DR3 NOD mice produced more Th1 associated immunoglobulin after immunization

To investigate the B-cell response to immunization, we tested serum Ig isotypes in HLA-DR3 mice immunized with autoantigen or control adjuvant. Immunization promoted the increase of most of the Ig isotypes IgG2a, a classical Th1 driven isotype was the only isotype significantly higher in antigen-immunized mice compared with the control group (Fig. 6).

Author Manuscript Author Manuscript Author Manuscript Author Manuscript

Immunized HLA-DR3 and WT NOD mice have a distinct gut microbiota

Recent studies have suggested that gut microbiota play an important role in health and disease including autoimmune disorders (39). To investigate whether gut microbiota was involved in the present AIH model induced by autoantigen immunization, we performed 16S rRNA sequencing of the fecal samples collected from HLA-DR3 and WT NOD mice 6 months after CYP2D6/FTCD immunization, at the peak of the ALT levels. It is intriguing that the composition of gut microbiota in HLA-DR3 mice was strikingly different from that of the WT NOD mice immunized with the same antigen both in terms of phylogenic diversity (PD, or alpha diversity) (Fig. 7A) and beta diversity (Fig. 7B, principal component analysis, PCA). Taxonomic analysis also revealed that the difference was at various taxonomic classification levels (Fig. 7C).

Discussion

We have developed a novel ‘humanized’ mouse model of AIH through immunization of human HLA-DR3 transgenic NOD mice with CYP2D6/FTCD. Immunization with these liver autoantigens induces a chronic liver injury that closely mirrors human AIH, indicating that the human HLA-DR3 gene is crucial for the development of this disease.

After immunization with CYP2D6/FTCD, HLA-DR3 NOD mice developed anti-LKM1/anti-LC1 antibodies, the same autoantibodies in patients with AIH (40). Anti-LKM1/anti-LC1 were also present in control immunized WT NOD mice, a finding reminiscent of the C57BL/6 mouse model (20, 41), which produced a similar antigen specific humoral immune response after exposure to the CYP2D6/FTCD antigenic construct containing also IL-12. This is possibly due to the homology between murine and human FTCD (LC1) immunogen, whereas anti-LKM1 seen in the immunized mice is human specific as there is not a single equivalent protein to human CYP2D6 in mice (mouse CYP2D9 and/or CYP2D22, Lapierre, unpublished data). Of note, however, in our model the production of antigen-specific autoantibodies was significantly higher in HLA-DR3 immunized mice when compared to adjuvant treated controls, underscoring the importance of this autoimmunity predisposing HLA allele in the presentation of the autoantigen. The autoimmunity predisposing role of HLA-DR3 is further emphasized by the observation that HLA-DR3 immunized NOD mice developed the highest levels of ANA, an autoantibody characterizing AIH-1 but also present in patients with AIH-2 (5). The background autoantibody production in the control immunized WT NOD mice is likely to reflect the expression of multiple autoimmune susceptibility genes in this strain (24–26).

In our humanized mouse model of AIH the liver injury is particularly marked and reminiscent of the course of the human disease. Transaminase levels are significantly higher than controls starting from the third month post-immunization and increase steadily over time. This is accompanied by severe histological changes, including portal inflammation with prominent plasma cell infiltration, interface hepatitis, confluent necrosis and some fibrotic changes, which are features typical of the human disease. These changes are more severe than those reported in an earlier model where a similar CYP2D6/FTCD DNA (and IL-12) immunization approach was used in C57BL/6 mice (20), indicating a major role of HLA-DR3 in determining the full-blown disease phenotype.

Author Manuscript Author Manuscript Author Manuscript Author Manuscript

Phenotypical and functional data support a key role for cellular immunity in the pathogenesis of the autoimmune liver damage in our model. The HLA-DR3 NOD mice developed vigorous antigen-specific T-cell responses in parallel to biochemical and histological liver damage after autoantigen immunization. The lymphocytes from the antigen immunized HLA-DR3 mice mounted an antigen-specific response to the full CYP2D6/FTCD construct (by SLMNC) and its DR3 restricted epitopes (by SLMNC and LMNC). It is noteworthy that the epitope-specific response by LMNC was much stronger, although it was not statistical significant due to the variation. The likelihood that cellular immune responses are instrumental to severe liver damage in immunized HLA-DR3 NOD mice is supported by the finding of marked T-effector cell activation in their liver. Not only did these mice show an increase in hepatic cytotoxic CD8 T-cells, but the T-cells infiltrating the liver expressed strong Th1 and Th17, and weak Th2, profiles, as they produced more IFN-γ, TNF-α, and IL-17, and less IL-4 than the non-immunized controls. The predominant Th1 response was also mirrored by a significant increase of IgG2a levels, whose production is Th1 dependent.

The pathogenesis of autoimmune liver disease is multifactorial and the autoimmune attack of hepatocytes in AIH is reportedly facilitated by impaired immunoregulatory control by $CD4^+CD25^+FOXP3^+$ Tregs (42, 43). In this context it is of interest that the frequency of $Foxp3^+$ Tregs and their suppressive function are reduced along with florid inflammatory infiltrate in the HLA-DR3 mice. Similarly, low numbers of $Foxp3^+$ T-cells were found within the LMNC infiltrate in patients with active AIH (44). More relevant to the human disease, Lapierre et al have been able to improve liver damage, induced by FTCD immunization, by adoptive transfer of autologous Tregs in C57BL/6 mice (41).

The novelty of our model is that it combines the advances made by previous mouse models of AIH and human susceptibility gene HLA-DR3. First, we selected the well established autoantigen, human CYP2D6/FTCD fusion plasmid that was able to induce some liver damage, but the hepatic injury mediated by the autoantigen induced AIH in our HLA-DR3 mice is more severe (higher serum ALT level and autoantibodies, worse liver histopathology and impaired Tregs function). Second, it is known that NOD genetic background harbors multiple autoimmune susceptibility genes (24–26) and a recent study by Hardtke-Wolenski and colleagues confirmed that the liver damage was induced in NOD mice but not in C57BL/6 or FVB/N mice at 12 weeks after immunization with human FTCD coding adenovirus infection (21), Third, most of autoimmune disorders in humans are strongly associated with HLA-DR genes and Chella David's group has provided the *in vivo* evidence for the association with multiple sclerosis, rheumatoid arthritis and lupus using different transgenic C57BL/6 mice expressing HLA-DR2, HLA-DR3 and HLA-DR4 (27, 45, 46) amongst others. Using a similar approach, we also demonstrated the importance of HLA-DQ8 in autoimmune type 1 diabetes (T1D) *in vivo* (47) and the unexpected regulatory role HLA-DR4 in T1D (48). In these models, mice baring HLA-DR or DQ susceptibility gene had a stronger autoimmune phenotype compared to their wild type (WT) counterparts, elucidating the permissive role of particular HLA molecules in autoimmunity. In parallel, our current mouse model of AIH also evolved a stronger autoimmune response to CYP2D6/FTCD liver autoantigen in HLA-DR3 NOD mice compared to WT NOD mice.

Author Manuscript Author Manuscript Author Manuscript Author Manuscript

Another novelty of our current study is that we provide an important link between gut microbiota and AIH. While gut microbiota are known to play an important role in both health and disease, including autoimmune disorders (39, 49), little is known about their role in AIH, either in humans or in animal models. We found that the composition of gut microbiota in HLA-DR3 mice at the time of liver damage is significantly different from that of WT NOD mice. There is a reciprocal influence between the gut microbiota and the adaptive immune system: whether the shaping of the microbiota due to the possession of HLA-DR3 is involved in the development of liver centered autoimmunity needs to be further investigated both in humans and animal models.

In summary, we have established a humanized HLA-DR3 mouse model that mirrors closely the biochemical, histological and chronically progressive course of human AIH. Our study supports the strong HLA-DR3 influence on the development of AIH, as confirmed in our recent AIH family study, where a higher frequency of homozygous DR3 was found in pediatric patients with AIH than in their first-degree healthy relatives (50). Moreover, our study indicates that gut microbiota may play an important role in AIH. This mouse model will provide opportunities not only for further elucidating the pathogenesis of AIH, but, more importantly, for evaluating the efficacy and safety of novel therapeutic interventions.

Supplementary Material

Refer to Web version on PubMed Central for supplementary material.

Acknowledgments

Financial Support

This work was funded by DK088181, DK092882 and DK100500 to LW. MY and IC were supported by the research grants from the family Lenaerts (Belgium) and the Departments of Hepatology and Gastroenterology Ghent University Hospital. YW was partly supported by Beijing Municipal Science & Technology Commission (Capital Characteristic Clinic Applied Research Project, Z151100004015081, China). HY was supported by Research Fund of Capital Health Development (2011-2018-05, China). P.L. holds a CIHR/Canadian Association for the Study of the Liver (CASL) hepatology fellowship and a Thomas F. Nealon, III Postdoctoral Research Fellowship from the American Liver Foundation.

We are grateful for XJ Zhang's dedicated care of the mice used in this study and the efforts of Dr. Xiaoyan Xiao for amplification and purification of the CYP2D6/FTCD plasmid used in the early phase of the study. We thank Dr. Leo van Grunsven for his advice on liver fibrosis related assays and Dr. F.S. Wong for critical reading the manuscript.

Abbreviations

NOD	non-obese-diabetic (mouse)
ALT	alanine transaminase
IL-17	interleukin 17
IL-10	interleukin 10
TNF-α	tumor necrotic factor alpha
IFN-γ	interferon gamma

Author Manuscript Author Manuscript Author Manuscript Author Manuscript

WT	wild type
LMNCs	liver mononuclear immune cells
SMNC	spleen mononuclear immune cells
Tregs	regulatory T cells
ANA	anti-nuclear autoantibodies
anti-LKM-1	anti-liver kidney microsomal type-1 autoantibodies
anti-LC1	anti-liver cytosol type-1 autoantibodies
CYP2D6	Cytochrome P450 protein
FTCD	formiminotransferase cyclodeaminase
HLA	Human Leukocyte Antigen

References

1. Manns MP, Czaja AJ, Gorham JD, Krawitt EL, Mieli-Vergani G, Vergani D, Vierling JM, et al. Diagnosis and management of autoimmune hepatitis. Hepatology. 2010; 51:2193–2213. [PubMed: 20513004]
2. Mieli-Vergani G, Vergani D. Autoimmune hepatitis. Nat Rev Gastroenterol Hepatol. 2011; 8:320–329. [PubMed: 21537351]
3. Mieli-Vergani G, Heller S, Jara P, Vergani D, Chang MH, Fujisawa T, Gonzalez-Peralta RP, et al. Autoimmune hepatitis. J Pediatr Gastroenterol Nutr. 2009; 49:158–164. [PubMed: 19561543]
4. Liberal R, Mieli-Vergani G, Vergani D. Clinical significance of autoantibodies in autoimmune hepatitis. J Autoimmun. 2013; 46:17–24. [PubMed: 24016388]
5. Couto CA, Bittencourt PL, Porta G, Abrantes-Lemos CP, Carrilho FJ, Guardia BD, Cancado EL. Antismooth muscle and antiactin antibodies are indirect markers of histological and biochemical activity of autoimmune hepatitis. Hepatology. 2013
6. Manns MP, Johnson EF, Griffin KJ, Tan EM, Sullivan KF. Major antigen of liver kidney microsomal autoantibodies in idiopathic autoimmune hepatitis is cytochrome P450db1. J Clin Invest. 1989; 83:1066–1072. [PubMed: 2466049]
7. Lapierre P, Hajoui O, Homberg JC, Alvarez F. Formiminotransferase cyclodeaminase is an organ-specific autoantigen recognized by sera of patients with autoimmune hepatitis. Gastroenterology. 1999; 116:643–649. [PubMed: 10029623]
8. Czaja AJ, Donaldson PT. Genetic susceptibilities for immune expression and liver cell injury in autoimmune hepatitis. Immunol Rev. 2000; 174:250–259. [PubMed: 10807521]
9. Djilali-Saiah I, Renous R, Caillat-Zucman S, Debray D, Alvarez F. Linkage disequilibrium between HLA class II region and autoimmune hepatitis in pediatric patients. J Hepatol. 2004; 40:904–909. [PubMed: 15158329]
10. Qiu DK, Ma X. Relationship between human leukocyte antigen-DRB1 and autoimmune hepatitis type I in Chinese patients. J Gastroenterol Hepatol. 2003; 18:63–67. [PubMed: 12519226]
11. Djilali-Saiah I, Fakhfakh A, Louafi H, Caillat-Zucman S, Debray D, Alvarez F. HLA class II influences humoral autoimmunity in patients with type 2 autoimmune hepatitis. J Hepatol. 2006; 45:844–850. [PubMed: 17050030]
12. Longhi MS, Hussain MJ, Kwok WW, Mieli-Vergani G, Ma Y, Vergani D. Autoantigen-specific regulatory T cells, a potential tool for immune-tolerance reconstitution in type-2 autoimmune hepatitis. Hepatology. 2011; 53:536–547. [PubMed: 21274874]

Author Manuscript Author Manuscript Author Manuscript Author Manuscript

13. Deshmukh US, Sim DL, Dai C, Kannapell CJ, Gaskin F, Rajagopalan G, David CS, et al. HLA-DR3 restricted T cell epitope mimicry in induction of autoimmune response to lupus-associated antigen SmD. J Autoimmun. 2011; 37:254–262. [PubMed: 21868195]
14. Rood MJ, van Krugten MV, Zanelli E, van der Linden MW, Keijsers V, Schreuder GM, Verduyn W, et al. TNF-308A and HLA-DR3 alleles contribute independently to susceptibility to systemic lupus erythematosus. Arthritis Rheum. 2000; 43:129–134. [PubMed: 10643708]
15. Howson JM, Rosinger S, Smyth DJ, Boehm BO, Group A-ES, Todd JA. Genetic analysis of adult-onset autoimmune diabetes. Diabetes. 2011; 60:2645–2653. [PubMed: 21873553]
16. Kordonouri O, Hartmann R, Charpentier N, Knip M, Danne T, Ilonen J. Genetic risk markers related to diabetes-associated autoantibodies in young patients with type 1 diabetes in berlin, Germany. Exp Clin Endocrinol Diabetes. 2010; 118:245–249. [PubMed: 20140847]
17. Waldenstrom J. The diagnostic importance of ACTH. Acta Endocrinol (Copenh). 1950; 5:235–242. [PubMed: 14799102]
18. Mori Y, Mori T, Yoshida H, Ueda S, Iesato K, Wakashin Y, Wakashin M, et al. Study of cellular immunity in experimental autoimmune hepatitis in mice. Clin Exp Immunol. 1984; 57:85–92. [PubMed: 6430615]
19. Tiegs G. Experimental hepatitis and role of cytokines. Acta Gastroenterol Belg. 1997; 60:176–179. [PubMed: 9260332]
20. Lapierre P, Djilali-Saiah I, Vitozzi S, Alvarez F. A murine model of type 2 autoimmune hepatitis: Xenoimmunization with human antigens. Hepatology. 2004; 39:1066–1074. [PubMed: 15057911]
21. Hardtke-Wolenski M, Fischer K, Noyan F, Schlue J, Falk CS, Stahlhut M, Woller N, et al. Genetic predisposition and environmental danger signals initiate chronic autoimmune hepatitis driven by CD4+ T cells. Hepatology. 2013; 58:718–728. [PubMed: 23475565]
22. Ehser J, Holdener M, Christen S, Bayer M, Pfeilschifter JM, Hintermann E, Bogdanos D, et al. Molecular mimicry rather than identity breaks T-cell tolerance in the CYP2D6 mouse model for human autoimmune hepatitis. J Autoimmun. 2013; 42:39–49. [PubMed: 23200317]
23. Holdener M, Hintermann E, Bayer M, Rhode A, Rodrigo E, Hintereder G, Johnson EF, et al. Breaking tolerance to the natural human liver autoantigen cytochrome P450 2D6 by virus infection. J Exp Med. 2008; 205:1409–1422. [PubMed: 18474629]
24. You S, Alyanakian MA, Segovia B, Damotte D, Bluestone J, Bach JF, Chatenoud L. Immunoregulatory pathways controlling progression of autoimmunity in NOD mice. Ann N Y Acad Sci. 2008; 1150:300–310. [PubMed: 19120317]
25. van Belle TL, Coppieters KT, von Herrath MG. Type 1 diabetes: etiology, immunology, and therapeutic strategies. Physiol Rev. 2011; 91:79–118. [PubMed: 21248163]
26. Lundholm M, Mayans S, Motta V, Lofgren-Burstrom A, Danska J, Holmberg D. Variation in the Cd3 zeta (Cd247) gene correlates with altered T cell activation and is associated with autoimmune diabetes. J Immunol. 2010; 184:5537–5544. [PubMed: 20400699]
27. Kong YC, Lomo LC, Motte RW, Giraldo AA, Baisch J, Strauss G, Hammerling GJ, et al. HLA-DRB1 polymorphism determines susceptibility to autoimmune thyroiditis in transgenic mice: definitive association with HLA-DRB1*0301 (DR3) gene. J Exp Med. 1996; 184:1167–1172. [PubMed: 9064334]
28. Bedossa P, Poynard T. An algorithm for the grading of activity in chronic hepatitis C. The METAVIR Cooperative Study Group. Hepatology. 1996; 24:289–293. [PubMed: 8690394]
29. Ishak K, Baptista A, Bianchi L, Callea F, De Groote J, Gudat F, Denk H, et al. Histological grading and staging of chronic hepatitis. J Hepatol. 1995; 22:696–699. [PubMed: 7560864]
30. Lapierre P, Beland K, Martin C, Alvarez F Jr, Alvarez F. Forkhead box p3+ regulatory T cell underlies male resistance to experimental type 2 autoimmune hepatitis. Hepatology. 2010; 51:1789–1798. [PubMed: 20232291]
31. Wang Y, Hu Y, Chao C, Yuksel M, Colle I, Flavell RA, Ma Y, et al. Role of IRAK-M in alcohol induced liver injury. PLoS One. 2013; 8:e57085. [PubMed: 23437317]
32. Tan Q, Majewska-Szczepanik M, Zhang X, Szczepanik M, Zhou Z, Wong FS, Wen L. IRAK-M deficiency promotes the development of type 1 diabetes in NOD mice. Diabetes. 2014; 63:2761–2775. [PubMed: 24696448]

Author Manuscript Author Manuscript Author Manuscript Author Manuscript

33. Ma Y, Bogdanos DP, Hussain MJ, Underhill J, Bansal S, Longhi MS, Cheeseman P, et al. Polyclonal T-cell responses to cytochrome P450IID6 are associated with disease activity in autoimmune hepatitis type 2. Gastroenterology. 2006; 130:868–882. [PubMed: 16530525]
34. Longhi MS, Meda F, Wang P, Samyn M, Mieli-Vergani G, Vergani D, Ma Y. Expansion and de novo generation of potentially therapeutic regulatory T cells in patients with autoimmune hepatitis. Hepatology. 2008; 47:581–591. [PubMed: 18220288]
35. Peng J, Narasimhan S, Marchesi JR, Benson A, Wong FS, Wen L. Long term effect of gut microbiota transfer on diabetes development. J Autoimmun. 2014; 53:85–94. [PubMed: 24767831]
36. Favier CF, Vaughan EE, De Vos WM, Akkermans AD. Molecular monitoring of succession of bacterial communities in human neonates. Appl Environ Microbiol. 2002; 68:219–226. [PubMed: 11772630]
37. Caporaso JG, Kuczynski J, Stombaugh J, Bittinger K, Bushman FD, Costello EK, Fierer N, et al. QIIME allows analysis of high-throughput community sequencing data. Nat Methods. 2010; 7:335–336. [PubMed: 20383131]
38. Van Beneden K, Mannaerts I, Pauwels M, Van den Branden C, van Grunsven LA. HDAC inhibitors in experimental liver and kidney fibrosis. Fibrogenesis Tissue Repair. 2013; 6:1. [PubMed: 23281659]
39. Wen L, Ley RE, Volchkov PY, Stranges PB, Avanesyan L, Stonebraker AC, Hu C, et al. Innate immunity and intestinal microbiota in the development of Type 1 diabetes. Nature. 2008; 455:1109–1113. [PubMed: 18806780]
40. Vitozzi S, Lapierre P, Djilali-Saiah I, Alvarez F. Autoantibody detection in type 2 autoimmune hepatitis using a chimera recombinant protein. J Immunol Methods. 2002; 262:103–110. [PubMed: 11983223]
41. Lapierre P, Beland K, Yang R, Alvarez F. Adoptive transfer of ex vivo expanded regulatory T cells in an autoimmune hepatitis murine model restores peripheral tolerance. Hepatology. 2013; 57:217–227. [PubMed: 22911361]
42. Longhi MS, Ma Y, Grant CR, Samyn M, Gordon P, Mieli-Vergani G, Vergani D. T-regs in autoimmune hepatitis-systemic lupus erythematosus/mixed connective tissue disease overlap syndrome are functionally defective and display a Th1 cytokine profile. J Autoimmun. 2013; 41:146–151. [PubMed: 23287048]
43. Grant CR, Liberal R, Holder BS, Cardone J, Ma Y, Robson SC, Mieli-Vergani G, et al. Dysfunctional CD39 regulatory T cells and aberrant control of T helper type 17 cells in autoimmune hepatitis. Hepatology. 2013
44. Ferri S, Longhi MS, De Molo C, Lalanne C, Muratori P, Granito A, Hussain MJ, et al. A multifaceted imbalance of T cells with regulatory function characterizes type 1 autoimmune hepatitis. Hepatology. 2010; 52:999–1007. [PubMed: 20683931]
45. Luckey D, Behrens M, Smart M, Luthra H, David CS, Taneja V. DRB1*0402 may influence arthritis by promoting naive CD4+ T-cell differentiation in to regulatory T cells. Eur J Immunol. 2014; 44:3429–3438. [PubMed: 25103892]
46. Khare M, Mangalam A, Rodriguez M, David CS. HLA DR and DQ interaction in myelin oligodendrocyte glycoprotein-induced experimental autoimmune encephalomyelitis in HLA class II transgenic mice. J Neuroimmunol. 2005; 169:1–12. [PubMed: 16194572]
47. Wen L, Wong FS, Burkly L, Altieri M, Mamalaki C, Kioussis D, Flavell RA, et al. Induction of insulitis by glutamic acid decarboxylase peptide-specific and HLA-DQ8-restricted CD4(+) T cells from human DQ transgenic mice. J Clin Invest. 1998; 102:947–957. [PubMed: 9727063]
48. Wen L, Chen NY, Tang J, Sherwin R, Wong FS. The regulatory role of DR4 in a spontaneous diabetes DQ8 transgenic model. J Clin Invest. 2001; 107:871–880. [PubMed: 11285306]
49. Wang JJ, Yang GX, Zhang WC, Lu L, Tsuneyama K, Kronenberg M, Vela JL, et al. Escherichia coli infection induces autoimmune cholangitis and anti-mitochondrial antibodies in non-obese diabetic (NOD). B6 (Idd10/Idd18) mice. Clin Exp Immunol. 2014; 175:192–201. [PubMed: 24128311]

Author Manuscript Author Manuscript Author Manuscript Author Manuscript

50. Wang P, Su H, Underhill J, Blackmore LJ, Longhi MS, Grammatikopoulos T, Okokon EV, et al. Autoantibody and human leukocyte antigen profiles in children with autoimmune liver disease and their first-degree relatives. J Pediatr Gastroenterol Nutr. 2014; 58:457–462. [PubMed: 24231645]

Author Manuscript Author Manuscript Author Manuscript Author Manuscript

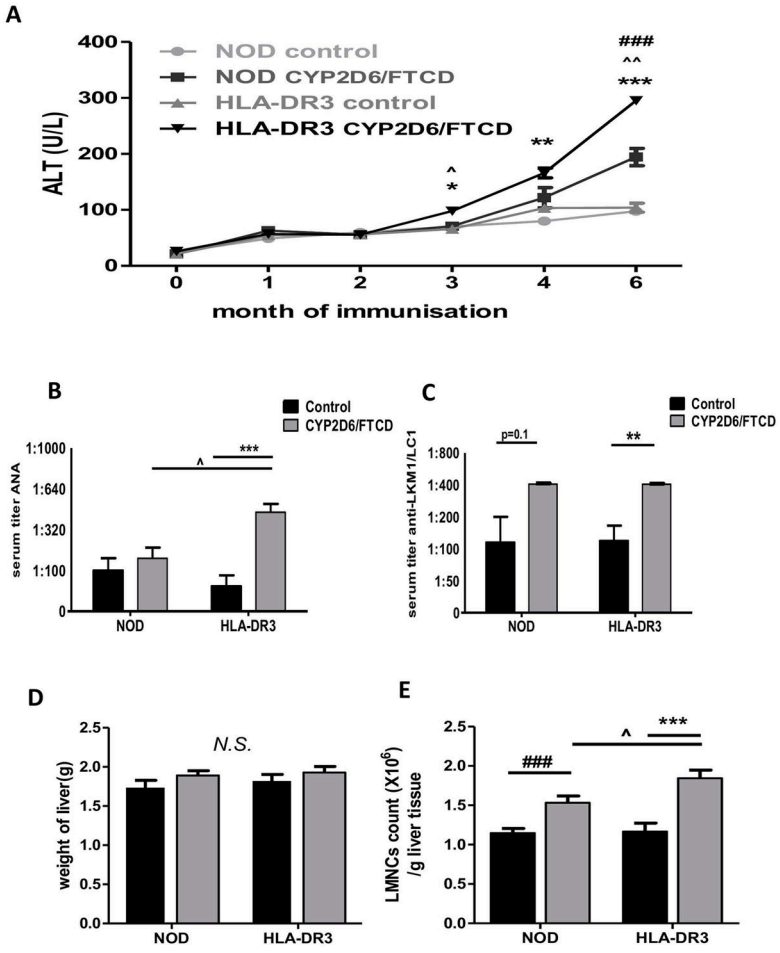

Fig. 1. Liver injury and immune cell infiltration

(A) Serum ALT levels: mice were bled at 0 (before immunization), 1, 2, 3, 4 and 6 months after immunization; (B) Serum ANA titer in mice 6 months after immunization with adjuvant (control, black bars) or CYP2D6/FTCD plasmid DNA plus adjuvant (gray bars). (C) Anti-LKM1/anti-LC1: the same serum samples were tested for anti-LKM1/anti-LC1 by an in house ELISA (30); (D) The liver weight of mice 6 months after immunization; (E) Liver mononuclear cells (LMNCs) count/gram liver tissue in mice 6 months after immunization. Error bars represent the SD of samples within a group. Symbol *= the comparison between HLA-DR3 control (adjuvant only) and HLA-DR3 CYP2D6/FTCD immunized mice; symbol ^= the comparison between HLA-DR3 and NOD mice immunized with CYP2D6/FTCD; symbol #= the comparison between adjuvant control and CYP2D6/FTCD immunized NOD mice. * (^ or #) $P<0.05$, ** (^^ or ##) $P<0.01$, *** (^^^ or ###) $P<0.001$.

Author Manuscript Author Manuscript Author Manuscript Author Manuscript

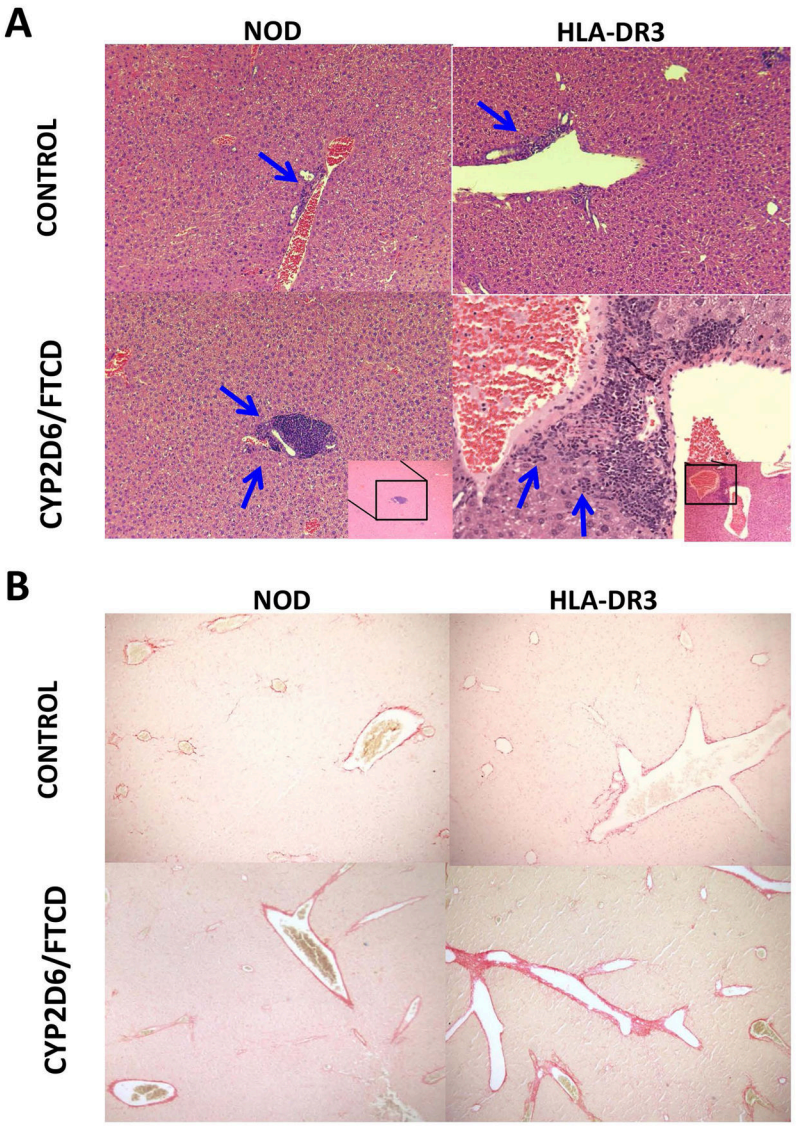

Author Manuscript Author Manuscript Author Manuscript Author Manuscript

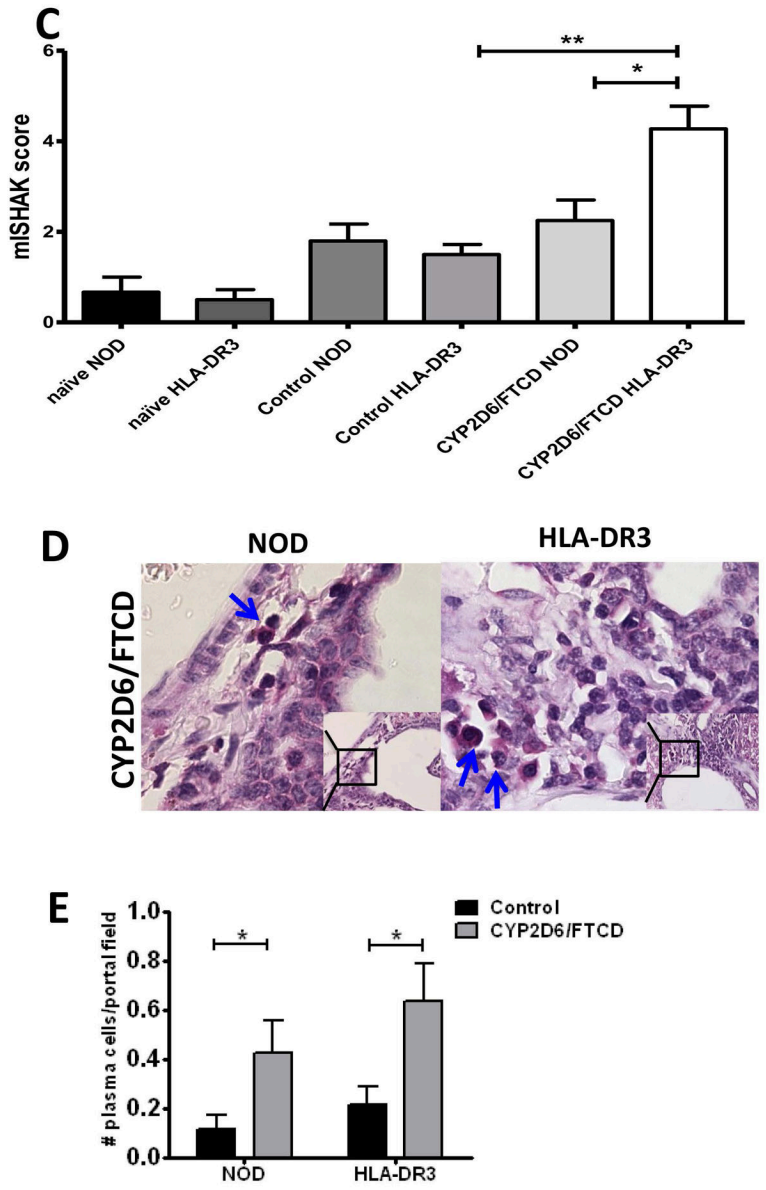

Fig. 2. Hepatic histology after immunization

Liver histology (six-month after immunization, H&E staining) was viewed under a light microscope (100X) by an investigator blinded to the experimental groups. (A) Histopathology of NOD control and NOD HLA-DR3 positive mice: a mild immune cell infiltration (blue arrows) is seen in both HLA-DR3 negative and positive control immunized mice; CYP2D6/FTCD immunized mice have marked mononuclear cell infiltration, which is particularly severe in HLA-DR3 mice, with interface hepatitis. (B) Sirius Red staining of fibrosis in control (adjuvant) and antigen CYP2D6/FTCD immunized NOD and HLA-DR3 mice; (C) mISHAK score to quantify liver damage; (D) Methyl-green pyronin staining for plasma cell detection, blue arrows show plasma cells in periportal area; (E) quantification of plasma cells. *p<0.05, non-parametric Student t test.

Author Manuscript Author Manuscript Author Manuscript Author Manuscript

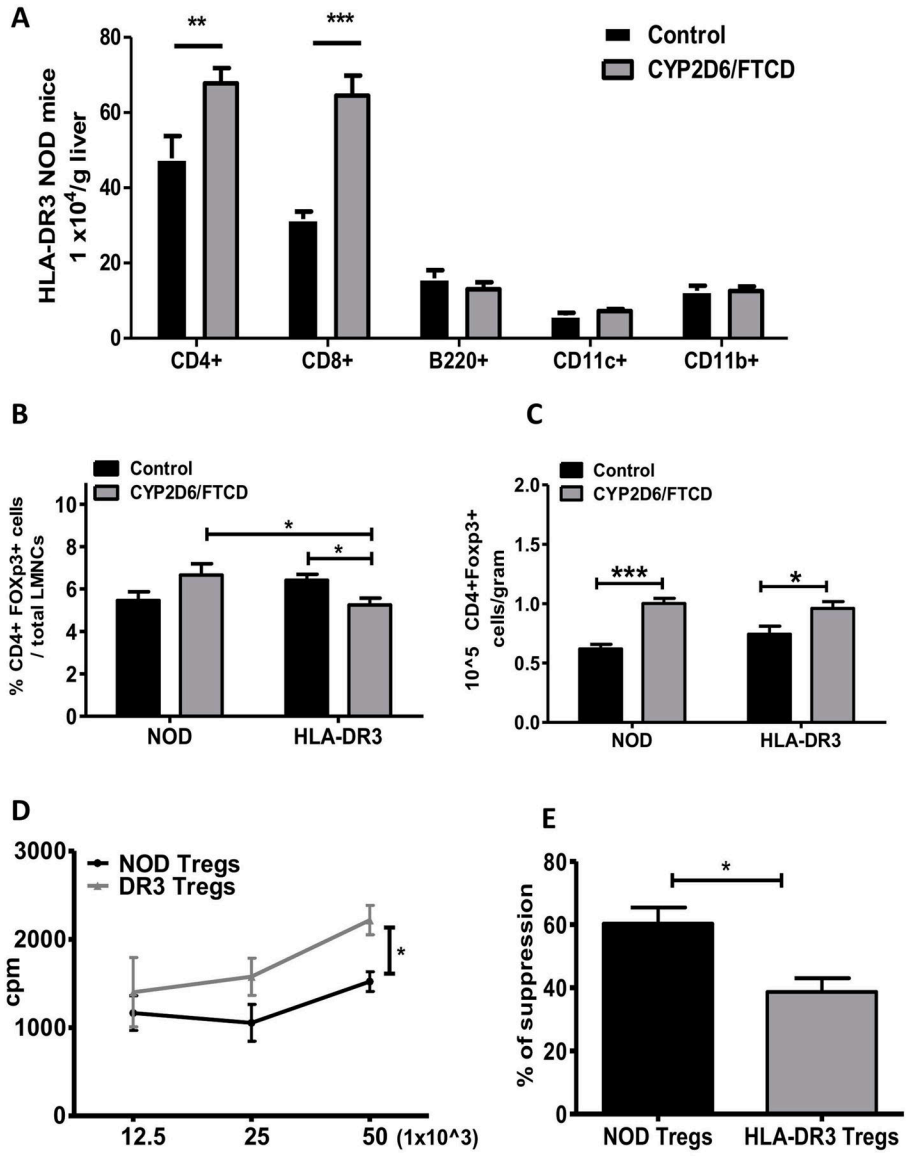

Fig. 3. Flow cytometric analysis of hepatic immune cell composition

Splenocytes and liver mononuclear cells (LMNCs) were isolated 6 months after immunization.

(A) composition of LMNCs from adjuvant control (black bars) and CYP2D6/FTCD immunized (gray bars) HLA-DR3 mice (n=6 group); (B+C) The frequency (left) and total number (right) of $CD4^{+}Foxp3^{+}$ Treg cells in LMNCs from control (black bars) and CYP2D6/FTCD immunized (gray bars) HLA-DR3 and WT NOD mice (n=6/group); (D) MLR proliferation with different allogen concentration; (E) Suppression of allogenic MLR by Treg cells (n=4/group). Error bars represent the SD of samples within a group. * $P<0.05$, ** $p<0.01$ and ***$P<0.001$ (non-parametric Student's t-test).

Author Manuscript Author Manuscript Author Manuscript Author Manuscript

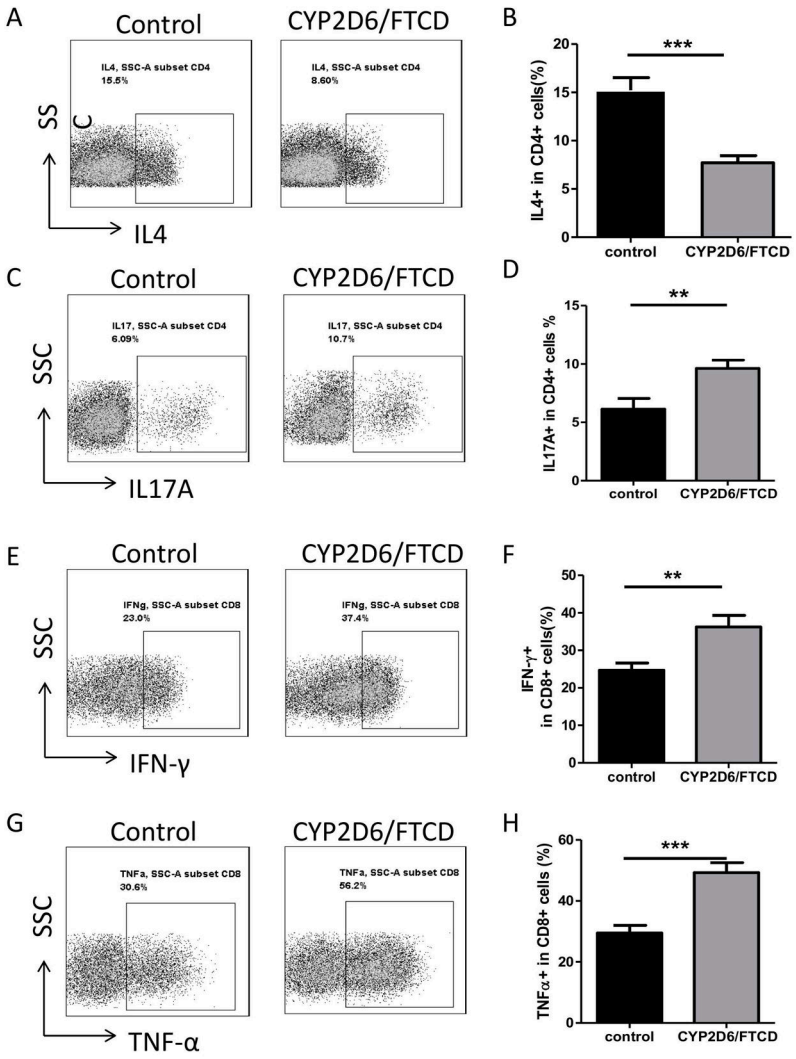

Fig. 4. Cytokine profile of LMNCs in HLA-DR3 mice after immunization

Ex vivo LMNCs of HLA-DR3 mice (n=6) were stained for intracellular cytokines. Representative FACS plots (A) and percentage (B) of IL-4$^+$ CD4$^+$ T-cells in adjuvant control and CYP2D6/FTCD immunized HLA-DR3 mice. Representative FACS plots (C) and percentage (D) of IL-17$^+$ CD4$^+$ T-cells in control and CYP2D6/FTCD immunized HLA-DR3 mice. Representative FACS plots (E) and percentage (F) of IFN-γ$^+$ CD8$^+$ T-cells in control and CYP2D6/FTCD immunized HLA-DR3 mice. Representative FACS plots (G) and percentage (H) of TNF-α$^+$ CD8$^+$ T-cells in control and CYP2D6/FTCD immunized HLA-DR3 mice. Error bars represent the SD of samples within a group. ***P*<0.01, ****P*<0.001 (non-parametric Student's t-test).

Author Manuscript Author Manuscript Author Manuscript Author Manuscript

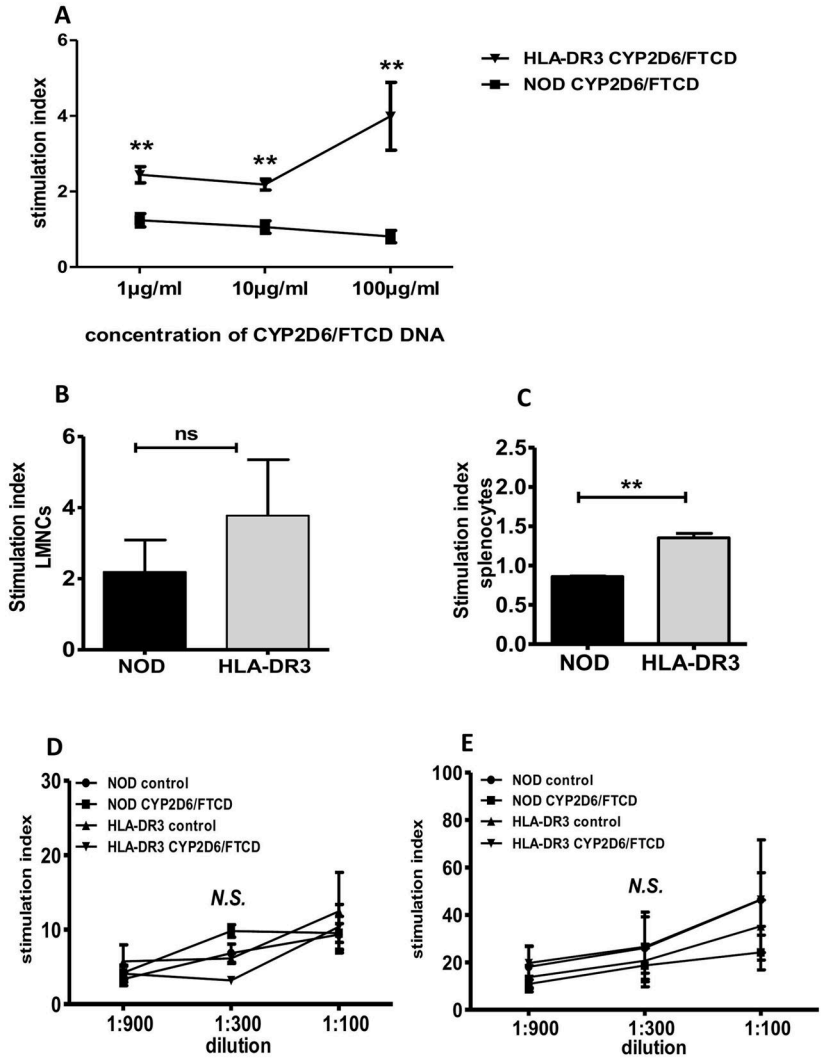

Fig. 5. T-cell response to hepatic autoantigen or anti-CD3 stimulation

Ex vivo T-cell response to CYD2D6/FTCD or anti-CD3 stimulation was tested in proliferation assays. (A) Antigen-specific splenic T-cell proliferation assay: $CD4^+$ T-cells were purified from CYP2D6/FTCD immunized WT or HLA-DR3 NOD mice and cultured with different concentrations of CYP2D6/FTCD plasmid DNA. The results are presented as T-cell stimulation index, (cpm with antigen/cpm without antigen); (B+C) LMNC or splenocytes T-cell response, to a mix (1:1) of DR3 restricted $CYP2D6_{313-332}$/ $CYP2D6_{393-412}$ in NOD or HLA-DR3 NOD mice; (D+E) non-antigen specific splenic T-cell proliferation to anti-CD3 only (D) and anti-CD3 plus anti-CD28 antibody (E). The concentration of anti-CD28 was 1:100 and the concentration of anti-CD3 is shown on the X-axis. Three to 4 mice were tested in each group. N.S.: not significant. ** $p<0.01$ (non-parametric Student's t-test).

Author Manuscript Author Manuscript Author Manuscript Author Manuscript

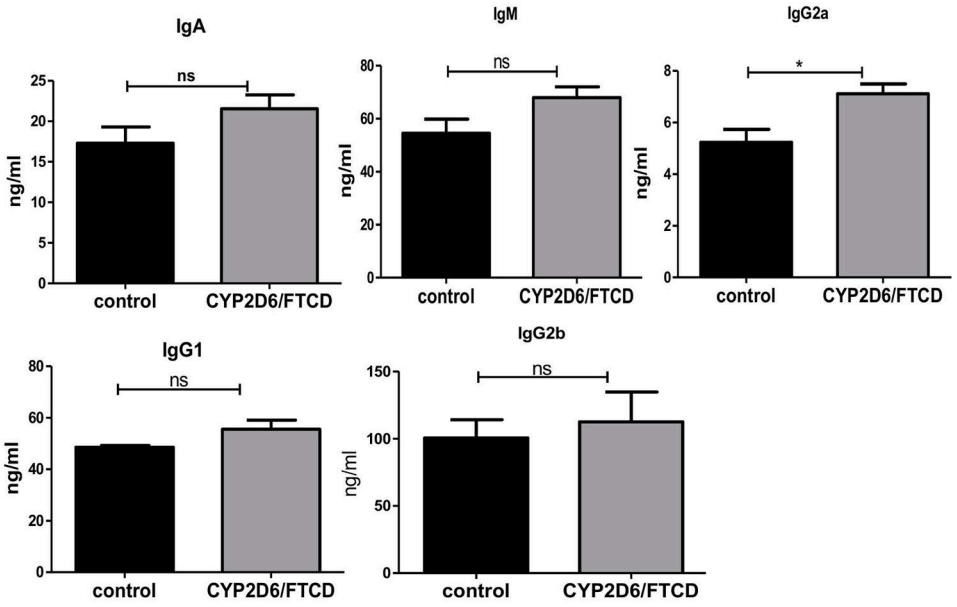

Fig. 6. Immunoglobulin (Ig) isotypes in HLA-DR3 NOD mice

Serum samples were taken from control (black bars) or CYP2D6 immunized (gray bars) HLA-DR3 NOD mice (6 months after immunization). Serum Ig of different isotypes was measured by ELISA. The samples were diluted at 1:1,000 and assayed in triplicate. The concentration of different isotypes was calculated based on the standard curves. N=4 mice/group were tested. NS: not significant; * $p<0.05$

Author Manuscript Author Manuscript Author Manuscript Author Manuscript

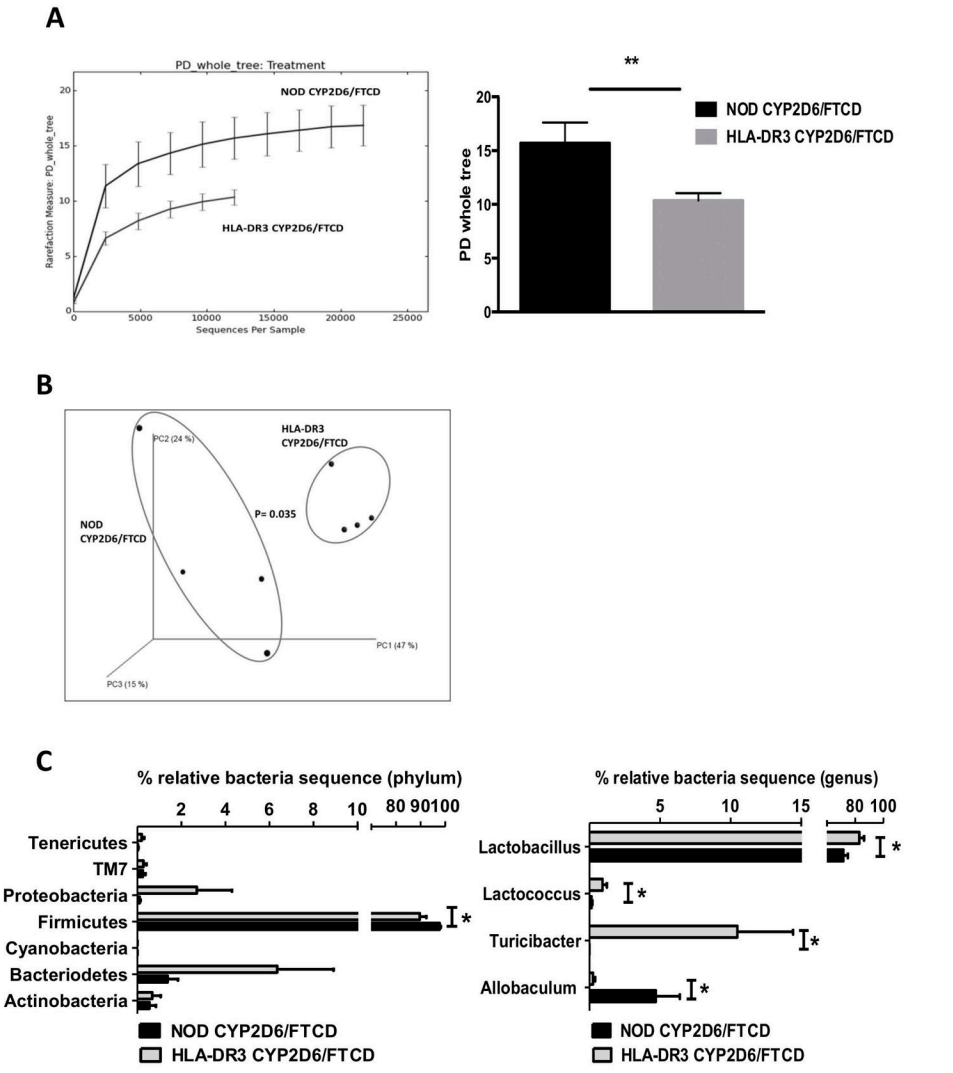

Fig. 7. The composition of gut microbiota in immunized NOD and HLA-DR3 NOD mice

Gut microbiota composition, in the fecal samples collected at 6 months after immunization from CYP2D6/FTCD immunized NOD and HLA-DR3 NOD mice, was examined by 16S rRNA deep-sequencing. (A) Alpha diversity of gut microbiota from NOD and HLA-DR3 mice was analyzed with QIIME software using a phylogenic diversity (PD) tree (left). NOD mice showed a significantly wider diversity of gut microbiota than HLA-DR3 mice (right); (B) Beta diversity of gut microbiota, analyzed with QIIME software using ANOSIM method for Principle Component Analysis (PCA); (C) Taxonomic analysis of representative gut bacteria at phylum (left) or genus (right) level from NOD and HLA-DR3 NOD mice. Four mice from each group were tested. *p<0.05 and **p<0.01.